Title: Structure of chitosan-ZnO layers electrophoretically deposited on NiTi shape memory alloy

Author: Tomasz Goryczka, Anna Kokoszka, Piotr Kowalski, Bożena Łosiewicz

Citation style: Goryczka Tomasz, Kokoszka Anna, Kowalski Piotr, Łosiewicz Bożena. (2016). Structure of chitosan-ZnO layers electrophoretically deposited on NiTi shape memory alloy. "Acta Physica Polonica. A" (Vol. 130, no. 4 (2016), s. 1056-1058), doi 10.12693/APhysPolA.130.1056

Proceedings of the XXIII Conference on Applied Crystallography, Krynica Zdrój, Poland, September 20–24, 2015

Structure of Chitosan–ZnO Layers Electrophoretically Deposited on NiTi Shape Memory Alloy

T. Goryczka*, A. Kokoszka, P. Kowalski and B. Łosiewicz
University of Silesia, Institute of Materials Science, Silesian Center for Education and Interdisciplinary Research, 75 Pułku Piechoty 1A, 41-500 Chorzów, Poland

The surface of NiTi shape memory was modified by deposition of chitosan–ZnO thin film. The electrodeposition process was carried out at room temperature at voltage-time conditions: 10 V/30 s, 10 V/300 s, 20 V/30 s, or 20 V/300 s. Structure of the obtained coatings was studied by means of grazing incidence beam X-ray diffraction. Distribution of the zinc oxide particles in the chitosan matrix was observed with use of scanning electron microscopy. It was found that depending on the electrodeposition parameters, the structure of the obtained chitosan–ZnO coatings varies from amorphous to coarse-grained.

DOI: 10.12693/APhysPolA.130.1056
PACS/topics: 61.10.Nz, 61.66.Dk, 68.37.Hk, 81.30.Kf, 87.68.+z

1. Introduction

The NiTi alloy with nickel content varying from 50.2 up to 51.0 at.% can be widely used in biomedical applications for implants as well as for part of medical tools and equipment [1]. The reason for that can be their unique properties — shape memory effects associated by reversible martensitic transformation [2]. The NiTi alloy reveals good biocompatibility, however, its corrosion resistance is still under improvement. Especially, attention is paid for elimination of the nickel ion release, which is considered as a toxic and/or carcinogenic element. In order to prevent shape memory effects, adaptation of the alloys goes in direction of their surface modification [3–5].

One of the ways can be covering of NiTi surface with a layer, which plays multi-functional role. On the one hand, they protect the NiTi alloy against corrosion. On the other hand, they increase osteointegration, reduce adhesion of bacteria as well as biofilm formation, etc. [1]. In our studies, surface of the NiTi shape memory alloy was electrophoretically covered with use of the composite consisted of chitosan (CH) matrix combined with ZnO particles as the composite component. Chitosan is a biocompatible polymer produced as a derivative of chitin. Due to its non-toxicity, stimulation of wound healing, preventing from infections, antimicrobial properties as well as biodegradability, it becomes used in medicine and veterinary [6–8].

Zinc oxide is one of the zinc compounds generally recognized as safe by the Food and Drug Administration (FDA). Thus why it is one of the most preferred materials for medical applications. Zinc is an essential micronutrient playing important roles in the development of humans and animal body. ZnO is a kind of activator supporting the rebuilding of the dentin, since the effect of reducing the degradation of collagen and increase of the durability of the resin used for its restore. Furthermore, because of their stability and antibacterial activity ZnO particles have a high potential to become a new generation of biocides [9–11].

2. Experimental data

Commercial NiTi alloy with chemical composition of 50.6 at.% Ni and 49.4 at.% Ti (Memry, Belgium) was used as a substrate for layer deposition. Firstly, the samples (15 mm × 8 mm × 0.8 mm) were cut from the NiTi alloy and quenched from 900 °C after 30 min of ageing. Then, their surface was mechanically polished using suspension with gradation down to 1 µm.

The basic component for production of the CH/ZnO coating was commercial powder of chitosan (Sigma-Aldrich) with 75–85% degree of deacetylation. Second components for layer preparation was zinc acetate (Acros Organics) with purity of 99%.

The layer CH/ZnO on surface of the NiTi alloy was produced using electrophoretic deposition process (EPD) with voltage of 10 V or 20 V and time 30 s and 300 s, respectively [12, 13]. Deposition was carried out from bath, which consisted from solutions mixture: 1:1 aquatic solution of 1 mM zinc acetate and 1% aquatic solution of the acetic acid, in which the 1 g/dm^3 of chitosan was solved. The deposition was carried out at room temperature. During electrophoretic deposition, the ZnO was synthesized from the zinc acetate solution, which contained zinc cations and was co-deposited with chitosan on the NiTi surface.

The phase analysis was done basing on the X-ray diffraction patterns measured using X'Pert Pro diffractometer with Cu $K_{\alpha(1/2)}$ radiation. Measurements were

*corresponding author; e-mail: tomasz.goryczka@us.edu.pl

carried out at room temperature over a 2θ range of 5−140°. Diffraction patterns were registered using grazing incidence technique (GIXD) at constant alpha angle of: 0.2, 0.3, 0.5, 0.8, or 1.0 degree. Observation of the CH/ZnO layers was carried out with use of a JEOL JSM-6480 scanning electron microscopy. Attached energy dispersive spectrometer (EDS) was used for chemical analysis.

3. Results and discussion

3.1. Materials before layer deposition

The NiTi shape memory alloys reveal a presence of the reversible martensitic transformation, which occurs between the $B2$ parent phase (higher temperature phase) and the $B19'$ monoclinic martensite (low temperature phase). Quenching from 900 °C, done after 20 min annealing, provides the $B2$ phase at the room temperature. In a result of this thermal treatment, the martensite start temperature (M_s) is below –28 °C. Measured X-ray diffraction pattern proved the $B2$ parent phase at room temperature (Fig. 1 — blue line). All diffraction lines were identified as belonging to the $B2$ phase. The diffraction powder was also measured for chitosan flacks (average size about 500 µm) before its deposition on NiTi surface (Fig. 1 — red line). In theory, the crystal lattice of the chitosan can be described using orthorhombic system with relatively high values of the unit cell parameters a_0 = 11.87 Å, b_0 = 14.72 Å, c_0 = 10.42 Å [14]. The strongest diffraction lines are concentrated around 20° 2θ position creating broadened maximum. Second maximum is formed around position of 10° 2θ. Determined half width at half intensity maximum (FWHM) varied from 2.3° up to 2.6° dependently on the increase of the position of diffraction line.

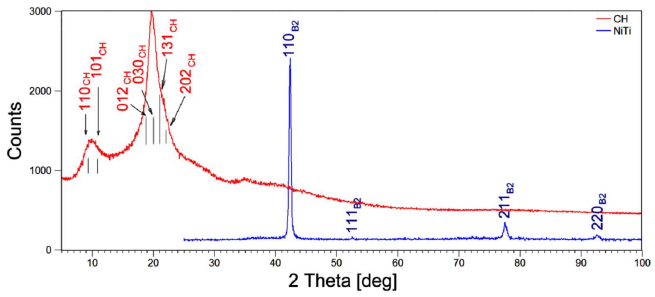

Fig. 1. X-ray diffraction patterns measured for chitosan (red line) and NiTi alloy (blue line) before layer deposition.

3.2. Structure of deposited composite

Results of the deposition process can be seen in Fig. 2. Scanning electron microscopy (SEM) images show surface of NiTi alloy coated by CH–ZnO layer using 10 V or 20 V with deposition time of 30 s or 300 s. In general, applied condition for deposition process caused thin film formation (consisting from chitosan) on surface of the NiTi alloy. Increasing the voltage or/and time resulted in agglomerates formation, which were covered by chitosan film. However, each processing condition brought specific formation of the ZnO agglomerates.

Application of the lowest deposition parameters (10 V/30 s) resulted in smooth layer formation without any cracks or pores. Increase of the deposition time up to 300 s caused formation of the ZnO agglomerates, which were sporadically formed at surface of the NiTi alloy in a shape of the islands. Further increase of the deposition voltage, up to 20 V, resulted in increase of the agglomerate amount at the coating. However, their shape was elongated and frayed. Deposition with shorter time (30 s) caused that the size of the agglomerates was lower and they were randomly distributed in the layer. Additional increase of the deposition time contributed in regular distribution of the ZnO agglomerates.

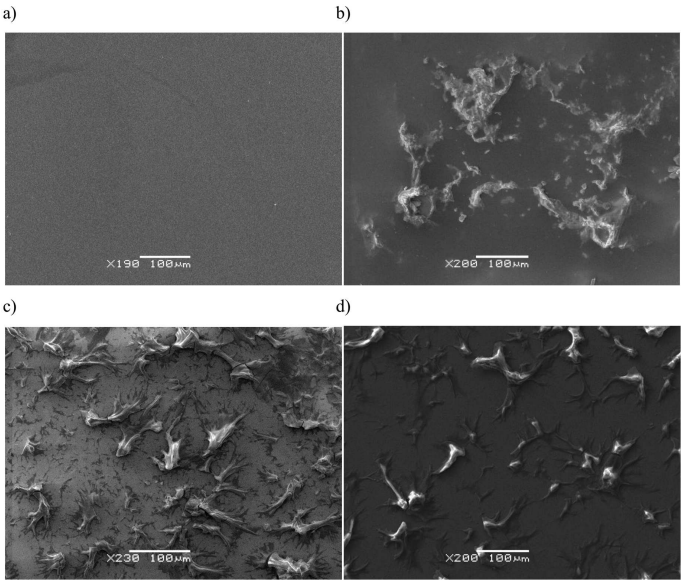

Fig. 2. SEM images observed for the CH–ZnO coatings deposited on the NiTi alloy at 10 V/30 s (a), 10 V/300 s (b), 20 V/30 s (c), and 20 V/300 s (d).

Deposited layer links the inorganic component, consisting of zinc and oxygen, as well as an organic biopolymer, which consists mainly of carbon and oxygen (Fig. 3). The analysis of chemical composition, done with use of EDS, revealed that film (formed at 10 V/30 s) contained evenly distributed zinc, oxygen as well as carbon inside of the coating. Also, the same distribution was stated in the area between agglomerates, when the coatings were deposited using higher voltage and longer deposition time. Concentration of zinc as well as oxygen significantly increased in agglomerates (Fig. 3b).

Previously obtained results were confirmed by the phase identification based on the measurement of the X-ray diffraction patterns. Figure 4 shows set of the X-ray diffraction patterns measured using GIXD tech-

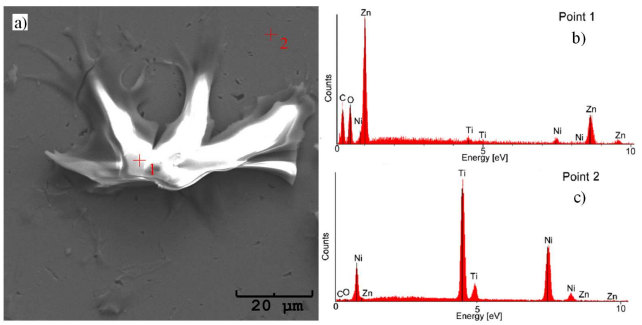

Fig. 3. SEM image (a) of the NiTi surface covered with CH/ZnO layer at 20 V/300 s and EDS spectra measured at point marked as "1" (b) and "2" (c).

nique (at constant alpha angle of 0.2 deg) for the lowest and highest condition of deposition process. For comparison, the X-ray diffraction pattern measured (the Bragg–Brentano geometry) for chitosan (initial state) was added. All diffraction patterns measured for layer deposited at applied processing condition contained weak diffraction lines (at position around 20° 2θ) which correspond to chitosan. Moreover, the substrate — NiTi alloy contained two phases: the $B2$ parent phase as well as monoclinic martensite — $B19'$. The monoclinic martensite can be induced (in depth of a few μm) during mechanical polishing of the substrate. The development of the ZnO phase dependently on the processing parameters can be discussed using $(111)_{ZnO}$ diffraction line (PDF-2 card no. 77-0191). Application of processing parameters 10 V/30 s caused formation of very low amount of the ZnO phase. In consequence of that very weak diffraction line appears at 2θ position of 36.32°. Further increase of processing parameters (voltage and deposition time) resulted in increase of the ZnO amount. Consequently, intensity of $(111)_{ZnO}$ diffraction line was stronger.

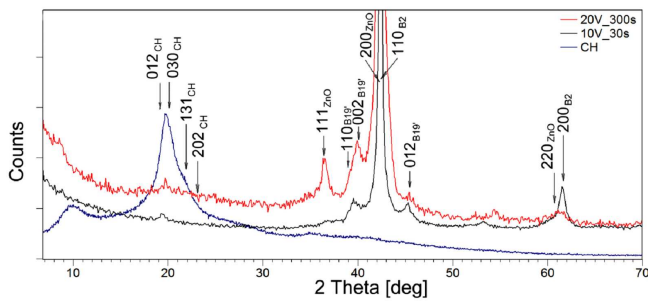

Fig. 4. Set of grazing incident diffraction patterns measured at constant alpha angle of 0.2 deg and diffraction pattern for pure chitosan measured at Bragg–Brentano geometry.

4. Conclusions

Obtained results can be summarized as follows:

1. The electrophoretic technique has been proved to be an effective technique to produce, in one single deposition process, composite coatings chitosan–ZnO on the surface of NiTi alloy.

2. The use of higher voltages leads to intensify the electrophoretic process and causes the expansion of the structure of the coating by increase of the size of agglomerates.

3. The parameters of the lower voltage allowed obtaining a chitosan coating surface–zinc oxide uniform, continuous smooth surface and the absence of areas with increased concentration of deposited components of the electrophoretic bath.

References

[1] L. Yahia, *Shape Memory Implants*, Springer-Verlag, Berlin 2000.

[2] T. Tadaki, K. Otsuka, K. Shimizu, *Ann. Rev. Mater. Sci.* **18**, 25 (1988).

[3] T. Goryczka, K. Dudek, B. Szaraniec, Ł. Zych, M. Freitag, J. Lelatko, *Eng. Biomater.* **106-108**, 124 (2011).

[4] J. Lelątko, T. Goryczka, T. Wierzchoń, M. Ossowski, B. Łosiewicz, E. Rowiński, H. Morawiec, *Solid State Phenom.* **163**, 127 (2010).

[5] K. Dudek, B. Szaraniec, J. Lelątko, T. Goryczka, *Solid State Phenom.* **203-204**, 90 (2013).

[6] H. Tang, P. Zhang, T.L. Kieft, S.H. Ryan, S.M. Baker, W.P. Wiesmann, S. Rogelj, *Acta Biomater.* **6**, 2562 (2010).

[7] E.I. Rabea, M.E. Badawy, C.V. Stevens, G. Smagghe, W. Steurbaut, *Biomacromolecules* **4**, 457 (2003).

[8] H. Ueno, T. Mori, T. Fujinaga, *Adv. Drug Deliv. Rev.* **52**, 105 (2001).

[9] H. Esmailzadeh, P. Sangpour, F. Shahraz, J. Hejazi, R. Khaksar, *Mater. Sci. Eng. C* **58**, 1058 (2016).

[10] S.M. Dizaj, F. Lotfipour, M. Barzegar-Jalali, M.H. Zarrintan, K. Adibkia, *Mater. Sci. Eng. C* **44**, 278 (2014).

[11] M. Cepin, G. Hribar, S. Caserman, Z.C. Orel, *Mater. Sci. Eng. C* **52**, 204 (2015).

[12] P. Kowalski, B. Łosiewicz, T. Goryczka, *Solid State Phenom.* **203-204**, 236 (2013).

[13] P. Kowalski, B. Łosiewicz, T. Goryczka, *Archiv. Metall. Mater.* **60**, 171 (2015).

[14] K. Ogawa, S. Inukai, *Carbohydr. Res.* **160**, 425 (1987).